

# QCD at high temperature and density: selected highlights

Jon-Ivar Skullerud<sup>1,\*</sup>

<sup>1</sup>*Department of Theoretical Physics, Maynooth University, Maynooth, Co Kildare, Ireland*

**Abstract.** I review some of the recent progress in QCD at high temperature and density, with a focus on the nature of the high-temperature transition; cold and dense matter; and hadron properties and transport coefficients at high temperature.

## 1 Introduction

Understanding the phase diagram of QCD and the properties of hot and dense strongly interacting matter is an endeavour of great scope and interest. Besides the theoretical interest in the exotic forms of matter that may appear under these conditions, a full understanding will cast light on the formation of matter in the early universe, the properties of neutron stars, the formation of heavy elements, and much more. Aligned to this is the experimental programme at RHIC and LHC and, in the near future, at FAIR and NICA.

The theoretical effort that has gone into this field over the past number of years is so large and varied that it will not be possible to do it full justice in one talk, and this overview is therefore necessarily selective. Important topics that will not be covered here include the QCD equation of state at high temperature, QCD in nonzero magnetic field, topology and deconfinement, non-equilibrium dynamics, and much more (see for example [1–5] for complementary overviews). I will instead focus on aspects of the transition(s) at zero chemical potential  $\mu$ ; exploring the chiral critical line at nonzero  $\mu$ ; some progress in understanding matter at large  $\mu$  and low temperature  $T$ ; and hadron properties and transport coefficients at large  $T$ . The emphasis will be on lattice QCD results, but not exclusively so: in particular, results using other Dyson–Schwinger equations (DSEs), the functional renormalisation group (FRG) and perturbation theory will be referenced where appropriate.

## 2 Transition(s) at zero chemical potential

### 2.1 Location and order of the chiral transition

It is by now well established that the transition from the hadronic phase to the quark–gluon plasma at  $\mu = 0$  is a crossover, characterised by a rapid change in the chiral condensate and a peak in the chiral susceptibility. Away from the chiral limit (where a true phase transition is expected) there is therefore no unique definition of the pseudocritical temperature  $T_c$ , but different definitions (e.g., the peak in the susceptibility  $T_\chi$  or the inflection point of the renormalised chiral condensate  $T_\Delta$ ) give compatible results for physical quark masses. There is also good agreement on the value of  $T_c$  at the physical

---

\*e-mail: jonivar.skullerud@mu.ie

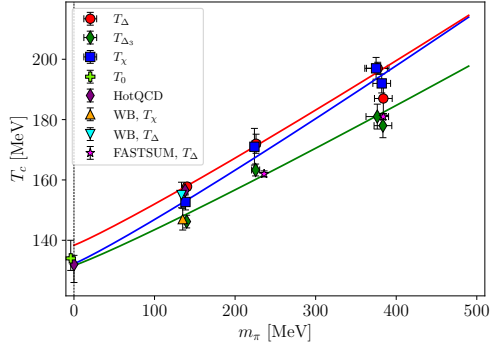


**Figure 1.** Pseudocritical temperature  $T_c$  as a function of the pion mass  $m_\pi$  from different lattice collaborations, from [8].

point between lattice groups using different fermion formulations [6–8] as well as with recent results from the DSE and FRG approaches [9, 10], with all finding  $T_\chi = 153 - 158$  MeV. Figure 1 [8] shows the mass dependence of  $T_c$  from different lattice calculations [6–8, 11] together with scaling functions, illustrating significant progress on the dependence of  $T_c$  on the light quark mass [8, 10, 12], leading to a critical temperature in the chiral limit  $T_0 = 130 - 140$  MeV.

The order of the chiral phase transition in the massless 2-flavour limit  $m_u, m_d \rightarrow 0$  is intimately connected with the fate of the anomalous  $U(1)_A$  symmetry. This symmetry is always broken by quantum effects, but if the breaking is small (*effective restoration*) at  $T_c$  the chiral transition may be first order or second order in the  $U(2)_L \otimes U(2)_R/U(2)_V$  universality class. On the other hand, if the symmetry remains strongly broken, the chiral transition will be second order in the  $O(4)$  universality class. Lattice studies have yet to arrive at a consensus on this issue, with [13–17] finding that the  $U(1)_A$  symmetry remains broken, while [18–21] finds that it is restored. It is worth noting that of these studies, only [16] has performed a continuum extrapolation. A recent FRG calculation [22] is consistent with  $U(1)_A$  restoration and an  $O(4)$  universality class.

The chiral transition is expected to be first order in the 3-flavour massless limit,  $m_u = m_d = m_s = 0$ . An open question is whether the transition is first or second order for physical strange quarks, and if it is first order, what is the critical pion mass  $m_\pi^c$  separating the first order transition region from the crossover region? The evidence from a number of lattice studies is that the first order region shrinks as the continuum limit is approached, with upper limits of  $m_\pi^c \lesssim 50$  MeV from highly improved staggered fermions [23] and  $m_\pi^c \lesssim 110$  MeV from Wilson–clover fermions [24]. A recent study with Wilson–clover fermions [25] found evidence of a first order transition, while no such evidence was found in a study using staggered fermions [26].

This question has also been addressed by studying systems with  $N_f > 3$ , where the first order transition in the chiral limit is expected to be stronger and persist to larger quark masses. Ohno *et al* [25] found evidence for a first order transition also for  $N_f = 4$  using Wilson–clover fermions. However, Cuteri *et al.* [27], performing a tricritical scaling analysis on staggered fermion data, found that the transition is consistent with second order. A reanalysis of Wilson–clover data gave the same result.

## 2.2 Some surprises

Recently, some intriguing evidence has emerged suggesting that the phase structure of QCD may be more complicated than previously thought, even at  $\mu = 0$ . In [28–30] it was found that in the region  $T_c < T \lesssim 3T_c$ , meson correlators exhibit certain degeneracies that are not present in the non-interacting case. This has been explained in terms of a chiral–spin symmetry  $SU(2)_{CS}$  and its flavour extension  $SU(2N_f)$ , which is a symmetry of the chromoelectric interaction, but is broken by the chromomagnetic interaction. Following this, it has been conjectured that the intermediate-temperature regime is a “stringy fluid” where chiral symmetry is restored and the chromomagnetic interaction is suppressed, but the confining chromoelectric field is still present.

Independently, it was found [31] that a condensate of thermal monopoles forms at roughly the same temperature in full ( $N_f = 2+1$ ) QCD as in pure gauge theory, where this coincides with the deconfinement transition, i.e., at roughly twice the chiral transition temperature. Furthermore, Alexandru and Horvath [32, 33] found an infrared scaling of the Dirac spectral density,  $\rho(\lambda) \propto 1/\lambda$ , which only set in at  $T > T_{IR} = 200 - 250 \text{ MeV} > T_c$ . They conjecture that this scaling is characteristic of a strongly coupled régime which only ends at a much higher (yet to be determined) temperature  $T_{UV}$ .

It is worth noting that the temperature scales for the suggested additional transitions are different, and that no connection between the different phenomena has been established. However, these results do point to the need for further investigations into the properties of QCD matter above  $T_c$ .

## 3 Chiral transition line

The shape of the transition line away from  $\mu = 0$  has been computed on the lattice using continuation from imaginary  $\mu$  [7, 34] and Taylor expansion [6, 34] (see also [35] for recent results using a novel reweighting method) as well as from Dyson–Schwinger equations [3], the functional renormalisation group [36] and a combination of the two [9, 37]. The pseudocritical temperature  $T_c(\mu_B)$  can be expanded in powers of  $\mu_B$ ,

$$\frac{T_c(\mu_B)}{T_c(0)} = 1 - \kappa_2 \left(\frac{\mu_B}{T_c}\right)^2 - \kappa_4 \left(\frac{\mu_B}{T_c}\right)^4 + \mathcal{O}(\mu_B^6) \quad (1)$$

leaving the parameters  $\kappa_2, \kappa_4$  and any higher order parameters to be determined. All the calculations have found that  $\kappa_4$  is consistent with zero within errors. Results for  $\kappa_2$  are shown in figure 2. All the lattice results shown have been continuum extrapolated and are consistent with each other. The most recent results from functional methods are also seen to be converging on the same values.

The right panel of figure 2 shows a summary [9] of lattice, functional and experimental data for the chiral transition and freezout curves. In [9] their DSE/FRG calculations were found to be reliable up to  $\mu_B/T = 3$ , which means that the location of the critical endpoints shown in the figure should only be considered indicative, and the spread between the different results reflect the remaining systematic uncertainties in the approaches.

Fluctuations and correlations of the conserved quantum numbers (baryon number  $B$ , electric charge  $Q$  and strangeness  $S$ ) play a crucial rôle in connecting theoretical predictions with experimental results. From the generalised susceptibilities,

$$\chi_{i,j,k}^{B,Q,S} = \frac{\partial^{i+j+k}(p/T^4)}{(\partial\hat{\mu}_B)^i(\partial\hat{\mu}_Q)^j(\partial\hat{\mu}_S)^k}, \quad \hat{\mu}_a \equiv \frac{\mu_a}{T} \quad (2)$$

we may compute experimentally observable quantities such as the mean  $M_B = \chi_1^B$ , variance  $\sigma_B^2 = \chi_2^B$ , skewness  $S_B = \chi_3^B/(\chi_2^B)^{3/2}$  and kurtosis  $\kappa_B = \chi_4^B/(\chi_2^B)^2$  of the baryon number distribution. Cumulants

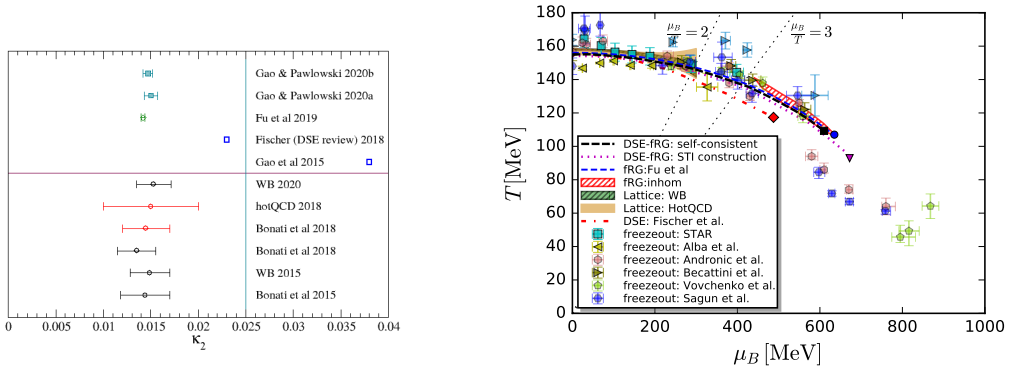


**Figure 2.** Left: The curvature parameter  $\kappa_2$  from lattice QCD [6, 7, 34, 38, 39] (bottom panel) and functional methods (blue: DSE, green: FRG) [3, 9, 36, 37, 40] (top panel). Black points have been obtained by analytic continuation from imaginary  $\mu$ , while red points are from Taylor expansion. Right: Transition line and critical endpoint from lattice and functional methods together with experimental freezeout lines, from [9].

up to 8th order have been computed by the Wuppertal–Budapest collaboration [41] and the HotQCD collaboration [42] and used to determine skewness and kurtosis at nonzero baryon chemical potential as well as preliminary results for the hyper-kurtosis (the sixth moment of the distribution). Results have also been obtained in the FRG framework using a low-energy effective theory [43, 44]. These results may in turn be used to extract freezeout parameters from experimental data and check whether experimental results are consistent with equilibrium QCD.

## 4 Large density

The methods employed to map out the phase diagram at high  $T$  and small  $\mu$  break down at lower temperature, in particular in the region relevant to nuclear matter and the interior of neutron stars. Recent progress has been made with several alternative methods including complex Langevin simulations, Lefschetz thimble-based methods [45], density of states [46, 47] and strong coupling expansions [48]. In addition, QCD-like theories where the sign problem is absent or weak may serve as a laboratory for generic features of gauge theories at high density as well as provide checks on the validity of other methods. Finally, perturbation theory, valid at asymptotically high densities, can provide constraints on physics at intermediate densities. In the following only a few selected highlights will be presented.

Complex Langevin methods have now reached the point where they have been used to simulate fully dynamical QCD with pion masses down to  $\sim 500$  MeV [49–51]. Figure 3 shows the fermion density as a function of the chemical potential from a simulation with  $N_f = 2$  Wilson fermions with  $m_\pi \approx 500$  MeV and a lattice spacing  $a \approx 0.06$  fm [51]. At low temperature the Silver Blaze phenomenon is clearly seen, as the density remains zero up to  $\mu = m_N/3$  with an onset of nuclear matter beyond this point. At very high chemical potential we observe saturation, where all available fermion states on the lattice are occupied.

Recent developments in strong coupling methods [48], based on a character expansion of the gauge field action, have allowed simulations to be carried out for heavy quarks (using a hopping parameter expansion) [53] as well as for light quarks (using a dual formulation) [54, 55]. Recently, a continuous-time formulation for staggered fermions has been developed [52]. Figure 3 shows results

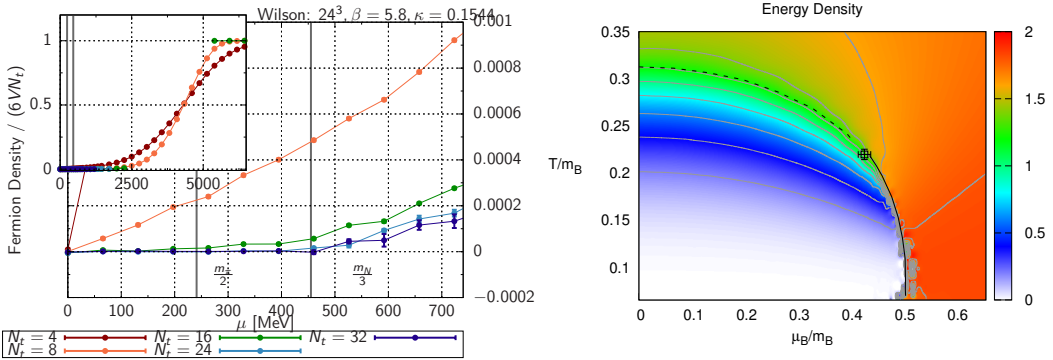


**Figure 3.** Left: Fermion density as function of chemical potential from complex Langevin with  $N_f = 2$  Wilson fermions [51], at temperatures ranging from 100 MeV ( $N_t = 32$ ) to 800 MeV ( $N_t = 4$ ). Right: Energy density as a function of temperature and chemical potential in the strong coupling expansion, from [52]. A first order nuclear gas–liquid transition with a critical endpoint is observed.

using this formulation, exhibiting a first-order nuclear gas–nuclear liquid phase transition including a critical endpoint. The strong coupling expansion has also been applied to large- $N_c$  QCD in the heavy dense limit [56], with findings consistent with the appearance of quarkyonic matter at large  $N_c$ .

QCD with nonzero isospin chemical potential  $\mu_I$  [57, 58] and two-colour QCD (QC<sub>2</sub>D) [59–63] do not suffer from the sign problem and are amenable to direct simulations at large density, and may hence provide benchmarks for other methods [64–69]. Both feature a superfluid phase for  $\mu_{I,B} > m_\pi$  characterised by condensation of pions and scalar diquarks respectively. The phase diagrams for both theories turn out to be remarkably similar; in particular, the superfluid transition temperature has been found to be almost independent of  $\mu$  in both cases. In QC<sub>2</sub>D simulations with different lattice formulations have found consistent results for the superfluid transition and have also confirmed the existence of a “quarkyonic” phase at large  $\mu$ , where quarks remain confined but the bulk degrees of freedom are weakly interacting quarks. A BEC régime described by chiral perturbation theory has been found at lower  $\mu$  for sufficiently light quarks [60]. It remains an open question whether there is a large- $\mu$  deconfinement transition at small temperature.

In the absence of reliable, non-perturbative, first-principles information on cold high-density matter, constraints can be placed by combining information on the nuclear matter equation of state with compact star observations. This may be further constrained by requiring the equation of state to match on to perturbation theory at very high density, which has recently been computed to NNLO including NNNLO terms [70]. This approach has been pursued in [70–74]. Specifically, the low-energy equation of state has been computed in a chiral EFT, with the EoS at intermediate density modelled by piecewise polytropes,  $p \propto n^\gamma$ . Typically, the polytropic index  $\gamma \sim 2.5$  for nuclear matter, while high-density perturbation theory corresponds to  $\gamma \in [0.5, 0.8]$ . Combined with recent observational data including from gravitational waves and the NICER observatory [74] only a subset of all possible equations of state remain. A result of such an analysis [71] is shown in figure 4, where it is concluded that stars with a mass  $2M_\odot$  will include a quark matter core, characterised by a small polytropic index, for any EoS that is not ruled out by observations.

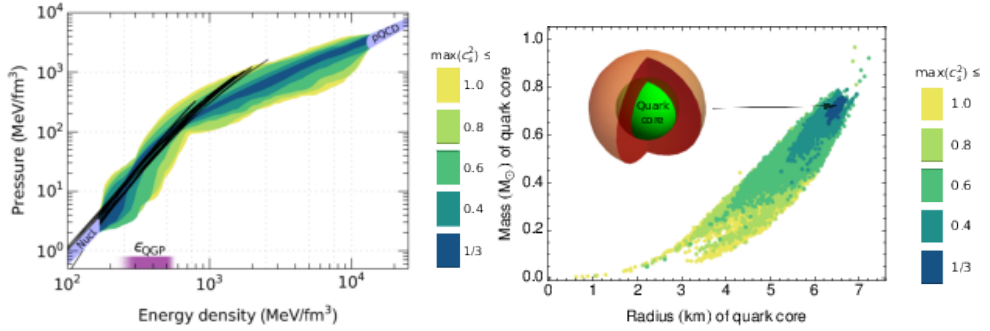


**Figure 4.** Left: Equation of state for high-density QCD obtained by interpolating between a nuclear eos (bottom left hand corner) and perturbative QCD (top right), constrained by mass and radius data from compact star observations. The kink in the eos suggests a transition from nuclear matter to quark matter. Right: The size of the quark matter core in a  $2M_{\odot}$  star, for the different interpolations shown in the left hand plot. Figures taken from [71].

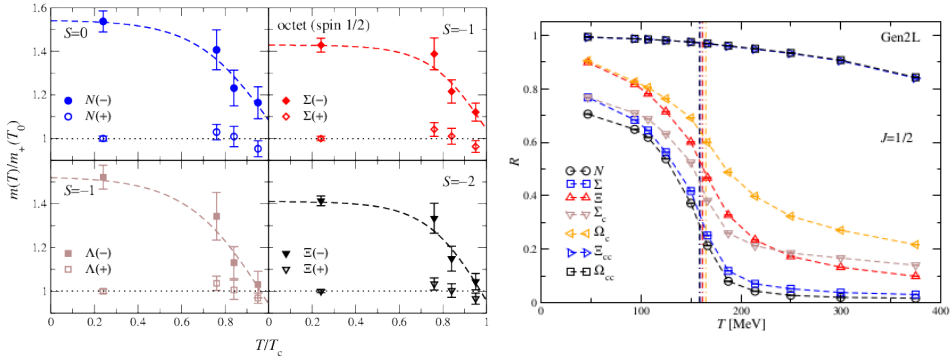


**Figure 5.** Left: Masses of positive and negative parity octet baryons below the deconfinement transition, from [75]. Right: The parity-doubling  $R$  parameter (3) for light, strange and charmed baryons.

## 5 Hadron properties and transport

### 5.1 Baryons

The FASTSUM collaboration has studied the properties of baryons at high temperature [11, 75–77], and in particular the emergent degeneracy between positive and negative parity states. Since positive and negative parity are states encoded in the same correlator (as forward and backward moving states respectively), the parameter

$$R = \frac{\sum_{n=0}^{\beta/2-1} R(\tau_n)/\sigma^2(\tau_n)}{\sum_{n=0}^{\beta/2-1} 1/\sigma^2(\tau_n)} ; \quad R(\tau) = \frac{G(\tau) - G(\beta - \tau)}{G(\tau) + G(\beta - \tau)} \quad (3)$$

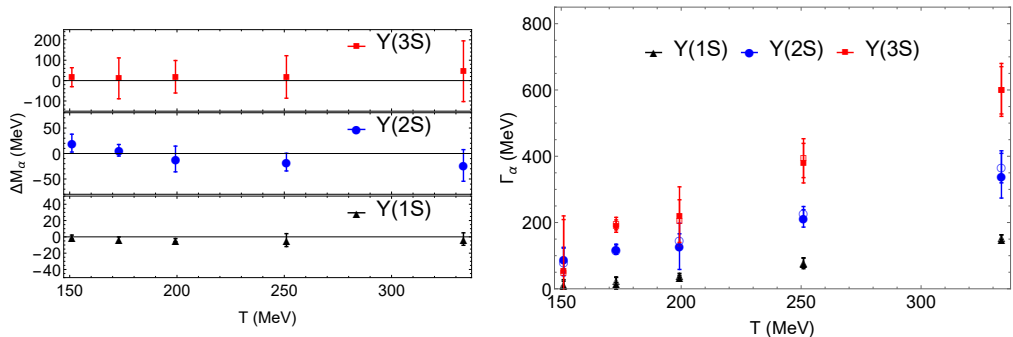


**Figure 6.** Mass shift (left) and width (right) for the  $\Upsilon$  1S, 2S and 3S states, from [79].

may serve as a measure of parity doubling, with  $R = 0$  when positive and negative parity states are completely degenerate. Figure 5 (left) shows the masses of positive and negative parity octet baryons below the deconfinement transition [77]: we see that while the masses positive-parity baryons remain unchanged, their negative-parity partners become lighter with increasing temperature with degeneracy setting in close to  $T_c$ , with potential impact on hadron resonance gas models [75]. The  $R$  parameter (3) is shown in figure 5 (right). It has an inflection point which is roughly the same for all light, strange and even singly-charmed baryons, and which coincides approximately with the chiral transition temperature [11]. Doubly-charmed baryons, however, do not appear sensitive to the chiral transition.

## 5.2 Heavy quarkonium

Heavy quarks have long been a focus of attention, both theoretically and experimentally, in the context of the quark–gluon plasma and heavy-ion collisions, see for example the review [78]. In recent years there has been significant progress towards a quantitative understanding of thermal mass shifts and widths of heavy quarkonia, in particular in the beauty sector. In a series of papers [79–81] Larsen *et al.* have employed lattice non-relativistic QCD (NRQCD) on hotQCD ensembles with  $N_f = 2 + 1$  and a near-physical pion mass. Using sources optimised to reproduce the zero-temperature spectrum and wavefunctions they have been able to fit the correlators to a gaussian plus low and high energy tails. The Bethe–Salpeter wavefunctions have also been determined [81]. Results for the vector ( $\Upsilon$ ) channel are shown in fig. 6, suggesting a very small (negative) mass shift for the ground state and a thermal width increasing with temperature as expected. Similar results are found for the P-wave  $\chi_{b0}$  (scalar) channel. It may be noted that a small negative mass shift has also been observed by Kim *et al.* [82] and for charmonium by Kelly *et al.* [83], both using the BR method [84].

These results need to be independently confirmed using different approaches. The FASTSUM collaboration has employed a wide range methods to determine the mass shift and width of the  $\Upsilon(1S)$  state [85], including Gaussian fits, moments of correlators, and spectral function reconstruction with linear, Bayesian and machine learning methods. The results are as yet inconclusive, revealing quite different systematics for the different methods, which need to be better understood.

The Bielefeld–CCNU collaboration has conducted a long series of studies of quarkonium in quenched QCD using nonperturbatively improved Wilson fermions. Their most recent results [86] suggest that there is no resonance peak above  $T_c$  for  $J/\psi$ , while the resonance peak for  $\Upsilon$  persists only up to  $1.5T_c$ . More work is clearly needed to understand the source of this discrepancy.

### 5.3 Transport

Transport properties describe the real-time, non-equilibrium properties of the medium, and are as such not directly accessible with the equilibrium methods of euclidean quantum field theory. However, a transport coefficient  $\kappa$  can be related to the spectral functions of the relevant conserved current  $J_\mu^k(x)$  via Kubo relations,

$$\kappa \propto \lim_{\omega \rightarrow 0} \frac{\rho^k(\omega)}{\omega}; \quad G_{ij}^k(\tau) = \int d^3x \langle J_i^k(\tau, \vec{x}) J_j^k(0, \vec{0}) \rangle = \frac{1}{2\pi} \int_0^\infty K(\omega, \tau; T) \rho_{ij}^k(\omega) d\omega, \quad (4)$$

where  $K(\omega, \tau; T)$  is a known integral kernel. While there has been some progress on shear and bulk viscosity [87, 88] and jet quenching [89, 90], we are still some way from obtaining quantitatively reliable predictions for these quantities, in contrast to the heavy quark diffusion coefficient and the electrical conductivity, which will be reviewed below.

Two methods have been used to compute the heavy quark diffusion coefficient from the lattice. One method [91] uses an effective theory where the heavy quark momentum diffusion coefficient is written in terms of a Polyakov loop correlator with a colour-electric field insertion. The main benefit of this method is that the related spectral function has a smooth behaviour as  $\omega \rightarrow 0$ , greatly reducing any uncertainties related to determining a potentially narrow transport peak. The main drawback is that the correlator is inherently noisy, and noise reduction techniques must be used to get a reasonable signal. Recent continuum extrapolated results from this method have been reported by TUMQCD [92], using a multilevel algorithm which is applicable for pure gauge theories, and by the Bielefeld–Darmstadt collaboration [93, 94] using the Wilson flow, which is also applicable in the presence of dynamical fermions. The results are consistent with each other and with earlier results [95, 96].

The second method uses fermionic vector correlators of charm and beauty quarks, with the benefit that finite quark mass effects are directly included, and the correlators are much less noisy than the gluonic correlators in the EFT method. The main drawback is that it can be very difficult to reliably determine the height of a possibly narrow transport peak. Continuum extrapolated results for both charm and beauty diffusion have recently been presented by the Bielefeld–CCNU collaboration [86].

Figure 7 (left) shows a comparison of lattice results for the diffusion coefficient  $D$  together with the NLO perturbative value. The results from each of the two methods are internally consistent, but the results from fermionic correlators are systematically smaller than from the effective field theory.

The electrical conductivity has been computed on the lattice by a number of groups using various approaches (see [98] for a recent review). In addition to earlier results with  $O(a)$  improved Wilson fermions and heavier than physical light quarks [99–101], there are now results using staggered fermions with physical up, down and strange quark masses [102, 103]. A summary of these results are shown in figure 7 (right panel). We see that there is good agreement between all the results despite the different methods used, suggesting that we are close to a quantitative, reliable determination of the conductivity of the QGP and its temperature variation. Astrakhantsev *et al.* have also computed the response of the conductivity to an external magnetic field [102] and to a nonzero baryon chemical potential [103]. The latter shows a reduction in the conductivity as  $\mu_B$  increases, in qualitative agreement with a direct calculation in two-colour QCD [61].

## 6 Summary

There has been a large amount of progress on understanding the properties of QCD at high temperature and density recently. In particular, we have reached the era of precision physics determining the chiral transition temperature  $T_c$  as well as the high-temperature equation of state, and we are within reach of



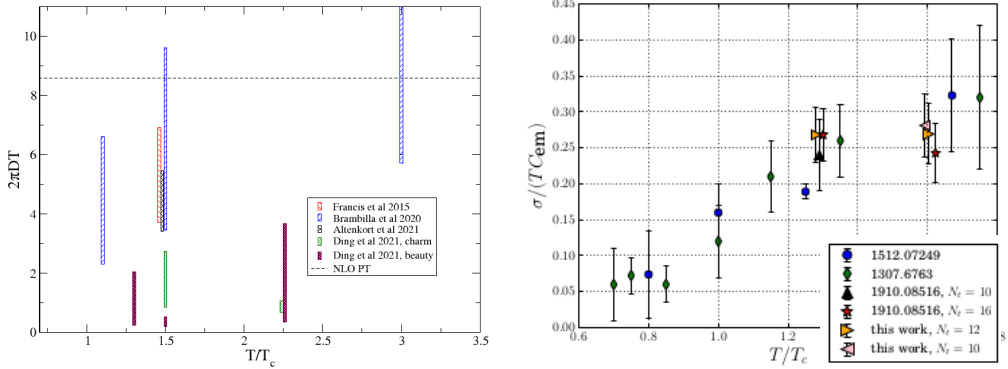


**Figure 7.** Left: summary of continuum-extrapolated lattice results for the heavy quark diffusion coefficient in pure gauge theory [86, 92–94, 96]. Hatched symbols are obtained using the EFT description; filled symbols are from fermionic operators. Right: Summary of lattice results for the electrical conductivity of QCD matter, from [97].

precision results for fluctuations both at zero and nonzero baryon density. We are also approaching a quantitative understanding of hadron properties in the hot medium as well as some transport properties, in particular the electrical conductivity. At the same time, despite significant progress especially in complex Langevin methods and constraints from compact star observations, we are far from being able to make reliable predictions in the low-temperature, high-density region relevant for neutron stars. First-principles calculations of the shear viscosity beyond theories with gravity duals are also in their infancy. Finally, the strong interaction has given us many surprises in the past and continues to surprise us in the present. It seems likely that there will be more surprises in store also in the future.

## References

- [1] K. Fukushima, C. Sasaki, *Prog. Part. Nucl. Phys.* **72**, 99 (2013), 1301.6377
- [2] H.T. Ding, *PoS LATTICE2016*, 022 (2017), 1702.00151
- [3] C.S. Fischer, *Prog. Part. Nucl. Phys.* **105**, 1 (2019), 1810.12938
- [4] J. Ghiglieri, A. Kurkela, M. Strickland, A. Vuorinen, *Phys. Rept.* **880**, 1 (2020), 2002.10188
- [5] J.N. Guenther, *Eur. Phys. J. A* **57**, 136 (2021), 2010.15503
- [6] A. Bazavov et al. (HotQCD), *Phys. Lett. B* **795**, 15 (2019), 1812.08235
- [7] S. Borsanyi, Z. Fodor, J.N. Guenther, R. Kara, S.D. Katz, P. Parotto, A. Pasztor, C. Ratti, K.K. Szabo, *Phys. Rev. Lett.* **125**, 052001 (2020), 2002.02821
- [8] A.Y. Kotov, M.P. Lombardo, A. Trunin, *Phys. Lett. B* **823**, 136749 (2021), 2105.09842
- [9] F. Gao, J.M. Pawłowski, *Phys. Lett. B* **820**, 136584 (2021), 2010.13705
- [10] J. Braun, W.j. Fu, J.M. Pawłowski, F. Rennecke, D. Rosenblüh, S. Yin, *Phys. Rev. D* **102**, 056010 (2020), 2003.13112
- [11] G. Aarts et al. (2020), 2007.04188
- [12] H.T. Ding et al. (HotQCD), *Phys. Rev. Lett.* **123**, 062002 (2019), 1903.04801
- [13] A. Bazavov et al. (HotQCD), *Phys. Rev. D* **86**, 094503 (2012), 1205.3535
- [14] M.I. Buchoff et al., *Phys. Rev. D* **89**, 054514 (2014), 1309.4149

- [15] V. Dick, F. Karsch, E. Laermann, S. Mukherjee, S. Sharma, Phys. Rev. D **91**, 094504 (2015), 1502.06190
- [16] H.T. Ding, S.T. Li, S. Mukherjee, A. Tomiya, X.D. Wang, Y. Zhang, Phys. Rev. Lett. **126**, 082001 (2021), 2010.14836
- [17] O. Kaczmarek, L. Mazur, S. Sharma (2021), 2102.06136
- [18] G. Cossu, S. Aoki, H. Fukaya, S. Hashimoto, T. Kaneko, H. Matsufuru, J.I. Noaki, Phys. Rev. D **87**, 114514 (2013), [Erratum: Phys.Rev.D 88, 019901 (2013)], 1304.6145
- [19] B.B. Brandt, A. Francis, H.B. Meyer, O. Philipsen, D. Robaina, H. Wittig, JHEP **12**, 158 (2016), 1608.06882
- [20] A. Tomiya, G. Cossu, S. Aoki, H. Fukaya, S. Hashimoto, T. Kaneko, J. Noaki, Phys. Rev. D **96**, 034509 (2017), [Addendum: Phys.Rev.D 96, 079902 (2017)], 1612.01908
- [21] S. Aoki, Y. Aoki, G. Cossu, H. Fukaya, S. Hashimoto, T. Kaneko, C. Rohrhofer, K. Suzuki (JLQCD), Phys. Rev. D **103**, 074506 (2021), 2011.01499
- [22] J. Braun, M. Leonhardt, J.M. Pawłowski, D. Rosenblüh (QCD) (2020), 2012.06231
- [23] A. Bazavov, H.T. Ding, P. Hegde, F. Karsch, E. Laermann, S. Mukherjee, P. Petreczky, C. Schmidt, Phys. Rev. D **95**, 074505 (2017), 1701.03548
- [24] Y. Kuramashi, Y. Nakamura, H. Ohno, S. Takeda, Phys. Rev. D **101**, 054509 (2020), 2001.04398
- [25] H. Ohno, Y. Kuramashi, Y. Nakamura, S. Takeda, *Critical endpoints in (2+1)- and 4-flavor QCD with Wilson-Clover fermions* (2021), presentation at Lattice 2021
- [26] S. Sharma, L. Dini, A. Lahiri, *Chiral phase transition temperature in 3-flavor QCD* (2021), presentation at Lattice 2021
- [27] F. Cuteri, O. Philipsen, A. Sciarra (2021), 2107.12739
- [28] C. Rohrhofer, Y. Aoki, G. Cossu, H. Fukaya, L.Y. Glozman, S. Hashimoto, C.B. Lang, S. Prelovsek, Phys. Rev. D **96**, 094501 (2017), [Erratum: Phys.Rev.D 99, 039901 (2019)], 1707.01881
- [29] C. Rohrhofer, Y. Aoki, G. Cossu, H. Fukaya, C. Gattringer, L.Y. Glozman, S. Hashimoto, C.B. Lang, S. Prelovsek, Phys. Rev. D **100**, 014502 (2019), 1902.03191
- [30] C. Rohrhofer, Y. Aoki, L.Y. Glozman, S. Hashimoto, Phys. Lett. B **802**, 135245 (2020), 1909.00927
- [31] M. Cardinali, M. D'Elia, A. Pasqui (2021), 2107.02745
- [32] A. Alexandru, I. Horváth, Phys. Rev. D **100**, 094507 (2019), 1906.08047
- [33] A. Alexandru, I. Horváth, Phys. Rev. Lett. **127**, 052303 (2021), 2103.05607
- [34] C. Bonati, M. D'Elia, F. Negro, F. Sanfilippo, K. Zambello, Phys. Rev. D **98**, 054510 (2018), 1805.02960
- [35] S. Borsanyi, Z. Fodor, M. Giordano, S.D. Katz, D. Nogradi, A. Pasztor, C.H. Wong (2021), 2108.09213
- [36] W.j. Fu, J.M. Pawłowski, F. Rennecke, Phys. Rev. D **101**, 054032 (2020), 1909.02991
- [37] F. Gao, J.M. Pawłowski, Phys. Rev. D **102**, 034027 (2020), 2002.07500
- [38] C. Bonati, M. D'Elia, M. Mariti, M. Mesiti, F. Negro, F. Sanfilippo, Phys. Rev. D **92**, 054503 (2015), 1507.03571
- [39] R. Bellwied, S. Borsanyi, Z. Fodor, J. Günther, S.D. Katz, C. Ratti, K.K. Szabo, Phys. Lett. B **751**, 559 (2015), 1507.07510
- [40] F. Gao, Y.x. Liu, Phys. Rev. D **94**, 076009 (2016), 1607.01675

- [41] S. Borsanyi, Z. Fodor, J.N. Guenther, S.K. Katz, K.K. Szabo, A. Pasztor, I. Portillo, C. Ratti, *JHEP* **10**, 205 (2018), 1805.04445
- [42] A. Bazavov et al., *Phys. Rev. D* **101**, 074502 (2020), 2001.08530
- [43] W.j. Fu, J.M. Pawłowski, F. Rennecke, B.J. Schaefer, *Phys. Rev. D* **94**, 116020 (2016), 1608.04302
- [44] W.j. Fu, X. Luo, J.M. Pawłowski, F. Rennecke, R. Wen, S. Yin (2021), 2101.06035
- [45] A. Alexandru, G. Basar, P.F. Bedaque, N.C. Warrington (2020), 2007.05436
- [46] K. Langfeld, *PoS LATTICE2016*, 010 (2017), 1610.09856
- [47] C. Gattringer, M. Mandl, P. Törek, *Phys. Rev. D* **100**, 114517 (2019), 1911.05320
- [48] O. Philipsen, *Strong coupling methods in QCD thermodynamics* (2021), 2104.03696
- [49] F. Attanasio, B. Jäger, F.P.G. Ziegler, *Eur. Phys. J. A* **56**, 251 (2020), 2006.00476
- [50] Y. Ito, H. Matsufuru, Y. Namekawa, J. Nishimura, S. Shimasaki, A. Tsuchiya, S. Tsutsui, *JHEP* **10**, 144 (2020), 2007.08778
- [51] F. Attanasio, B. Jäger, F.P.G. Ziegler, *With complex Langevin towards the QCD phase diagram, in 38th International Symposium on Lattice Field Theory* (2021), 2111.02241
- [52] M. Klegrewe, W. Unger, *Phys. Rev. D* **102**, 034505 (2020), 2005.10813
- [53] J. Glesaaen, M. Neuman, O. Philipsen, *JHEP* **03**, 100 (2016), 1512.05195
- [54] G. Gagliardi, J. Kim, W. Unger, *EPJ Web Conf.* **175**, 07047 (2018), 1710.07564
- [55] G. Gagliardi, W. Unger, *Phys. Rev. D* **101**, 034509 (2020), 1911.08389
- [56] O. Philipsen, J. Scheunert, *JHEP* **11**, 022 (2019), 1908.03136
- [57] B.B. Brandt, G. Endrődi, S. Schmalzbauer, *Phys. Rev.* **D97**, 054514 (2018), 1712.08190
- [58] B.B. Brandt, F. Cuteri, G. Endrődi, S. Schmalzbauer, *Particles* **3**, 80 (2020), 1912.07451
- [59] T. Boz, P. Giudice, S. Hands, J.I. Skullerud, *Phys. Rev. D* **101**, 074506 (2020), 1912.10975
- [60] N. Astrakhantsev, V.V. Braguta, E.M. Ilgenfritz, A.Y. Kotov, A.A. Nikolaev, *Phys. Rev. D* **102**, 074507 (2020), 2007.07640
- [61] P.V. Buividovich, D. Smith, L. von Smekal, *Phys. Rev. D* **102**, 094510 (2020), 2007.05639
- [62] K. Iida, E. Itou, T.G. Lee (2019), 1910.07872
- [63] J. Wilhelm, L. Holicki, D. Smith, B. Wellegehausen, L. von Smekal (2019), 1910.04495
- [64] J.O. Andersen, T. Brauner, W. Naylor, *Phys. Rev.* **D92**, 114504 (2015), 1505.05925
- [65] J. Chao, *Chin. Phys. C* **44**, 034108 (2020), 1808.01928
- [66] P. Adhikari, J.O. Andersen, *Phys. Lett. B* **804**, 135352 (2020), 1909.01131
- [67] T.G. Khunjua, K.G. Klimenko, R.N. Zhokhov, *JHEP* **06**, 148 (2020), 2003.10562
- [68] T. Furusawa, Y. Tanizaki, E. Itou, *Phys. Rev. Res.* **2**, 033253 (2020), 2005.13822
- [69] R. Contant, M.Q. Huber (2019), 1909.12796
- [70] T. Gorda, A. Kurkela, R. Paatelainen, S. Säppi, A. Vuorinen, *Phys. Rev. Lett.* **127**, 162003 (2021), 2103.05658
- [71] E. Annala, T. Gorda, A. Kurkela, J. Nättilä, A. Vuorinen, *Nature Phys.* **16**, 907 (2020), 1903.09121
- [72] E. Annala, T. Gorda, E. Katerini, A. Kurkela, J. Nättilä, V. Paschalidis, A. Vuorinen (2021), 2105.05132
- [73] S.K. Greif, K. Hebeler, J.M. Lattimer, C.J. Pethick, A. Schwenk, *Astrophys. J.* **901**, 155 (2020), 2005.14164
- [74] G. Raaijmakers, S.K. Greif, K. Hebeler, T. Hinderer, S. Nisanke, A. Schwenk, T.E. Riley, A.L. Watts, J.M. Lattimer, W.C.G. Ho, *Astrophys. J. Lett.* **918**, L29 (2021), 2105.06981
- [75] G. Aarts, C. Allton, D. De Boni, B. Jäger, *Phys. Rev.* **D99**, 074503 (2019), 1812.07393

- [76] G. Aarts, C. Allton, S. Hands, B. Jäger, C. Praki, J.I. Skullerud (2015), 1502.03603
- [77] G. Aarts, C. Allton, D. De Boni, S. Hands, B. Jäger, C. Praki, J.I. Skullerud, JHEP **06**, 034 (2017), 1703.09246
- [78] A. Rothkopf, Phys. Rept. **858**, 1 (2020), 1912.02253
- [79] R. Larsen, S. Meinel, S. Mukherjee, P. Petreczky, Phys. Lett. B **800**, 135119 (2020), 1910.07374
- [80] R. Larsen, S. Meinel, S. Mukherjee, P. Petreczky, Phys. Rev. D **100**, 074506 (2019), 1908.08437
- [81] R. Larsen, S. Meinel, S. Mukherjee, P. Petreczky, Phys. Rev. D **102**, 114508 (2020), 2008.00100
- [82] S. Kim, P. Petreczky, A. Rothkopf, JHEP **11**, 088 (2018), 1808.08781
- [83] A. Kelly, A. Rothkopf, J.I. Skullerud, Phys. Rev. **D97**, 114509 (2018), 1802.00667
- [84] Y. Burnier, A. Rothkopf, Phys. Rev. Lett. **111**, 182003 (2013), 1307.6106
- [85] T. Spriggs et al., *A comparison of spectral reconstruction methods applied to non-zero temperature NRQCD meson correlation functions*, these proceedings, 2112.04201
- [86] H.T. Ding, O. Kaczmarek, A.L. Lorenz, H. Ohno, H. Sandmeyer, H.T. Shu (2021), 2108.13693
- [87] N.Y. Astrakhantsev, V.V. Braguta, A.Y. Kotov, Phys. Rev. D **98**, 054515 (2018), 1804.02382
- [88] E. Itou, Y. Nagai, *QCD viscosity by combining the gradient flow and sparse modeling methods* (2021), presentation at Lattice 2021.
- [89] M. Panero, K. Rummukainen, A. Schäfer, Phys. Rev. Lett. **112**, 162001 (2014), 1307.5850
- [90] A. Kumar, A. Majumder, J.H. Weber (2020), 2010.14463
- [91] S. Caron-Huot, M. Laine, G.D. Moore, JHEP **04**, 053 (2009), 0901.1195
- [92] N. Brambilla, V. Leino, P. Petreczky, A. Vairo, Phys. Rev. D **102**, 074503 (2020), 2007.10078
- [93] L. Altenkort, A.M. Eller, O. Kaczmarek, L. Mazur, G.D. Moore, H.T. Shu, Phys. Rev. D **103**, 014511 (2021), 2009.13553
- [94] L. Altenkort, A.M. Eller, O. Kaczmarek, L. Mazur, G.D. Moore, H.T. Shu, *Spectral reconstruction details of a gradient-flowed color-electric correlator*, in *19th International Conference on Strangeness in Quark Matter* (2021), 2109.11303
- [95] D. Banerjee, S. Datta, R. Gavai, P. Majumdar, Phys. Rev. D **85**, 014510 (2012), 1109.5738
- [96] A. Francis, O. Kaczmarek, M. Laine, T. Neuhaus, H. Ohno, Phys. Rev. D **92**, 116003 (2015), 1508.04543
- [97] A. Trunin et al., *Electromagnetic conductivity of quark-gluon plasma at non-zero baryon density* (2021), presentation at Lattice 2021
- [98] G. Aarts, A. Nikolaev, Eur. Phys. J. A **57**, 118 (2021), 2008.12326
- [99] A. Amato, G. Aarts, C. Allton, P. Giudice, S. Hands, J.I. Skullerud, Phys.Rev.Lett. **111**, 172001 (2013), 1307.6763
- [100] G. Aarts, C. Allton, A. Amato, P. Giudice, S. Hands, J.I. Skullerud, JHEP **1502**, 186 (2015), 1412.6411
- [101] B.B. Brandt, A. Francis, B. Jäger, H.B. Meyer, Phys. Rev. D **93**, 054510 (2016), 1512.07249
- [102] N. Astrakhantsev, V.V. Braguta, M. D’Elia, A.Y. Kotov, A.A. Nikolaev, F. Sanfilippo, Phys. Rev. D **102**, 054516 (2020), 1910.08516
- [103] N. Astrakhantsev, V.V. Braguta, M. Cardinali, M. D’Elia, L. Maio, F. Sanfilippo, A. Trunin, A. Vasiliev, *Electromagnetic conductivity of quark-gluon plasma at non-zero baryon density*, in *38th International Symposium on Lattice Field Theory* (2021), 2110.10727